Escola de Camins
Escola Tècnica Superior d'Enginyeria de Camins, Canals i Ports
UPC BARCELONATECH

TREBALL FINAL DE MÀSTER

Assessing the impact of local emission abatement measures on ozone levels in Catalonia

Supplementary Material

Treball realitzat per:
Paula Camps Pla

Dirigit per:
Marc Guevara Vilardell
María Gonçalves Ageitos

Màster en:
Enginyeria Ambiental

Barcelona, 26 de setembre de 2023

Departament d'Enginyeria de Projectes i de la Construcció

Index

S.1. Trends of O_3 and NO_2 levels in Catalonia (2000-2021)

Figure S.1. Number of days exceeding the 120^{d8max} target value for the protection of human health at the available air quality stations in Catalonia from 2000 to 2021 (except 2000, 2003, 2019 and 2021, which are displayed in the main document of this thesis). The red vertical line shows the 25-day limit set in the Air Quality Directive.

(j) 2011

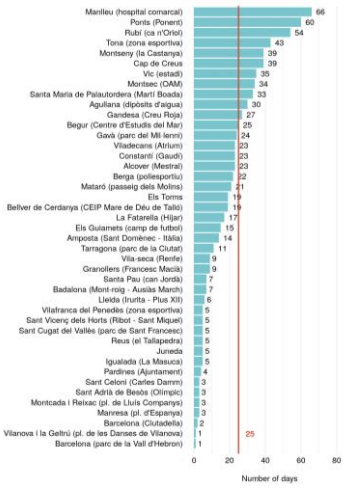

(k) 2012

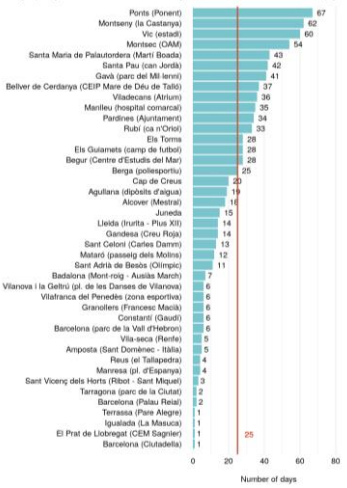

(l) 2013

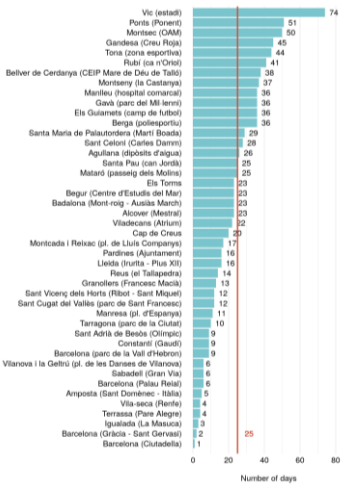

(m) 2014

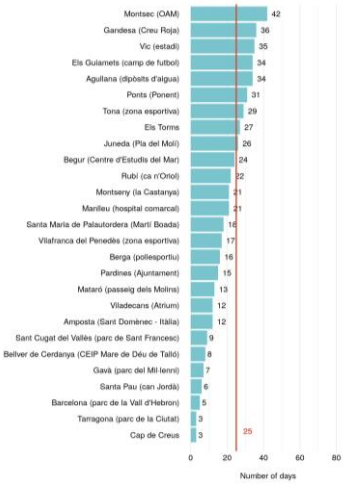

(n) 2015

(o) 2016

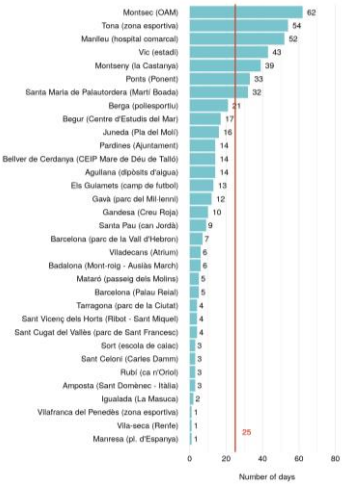

(p) 2017

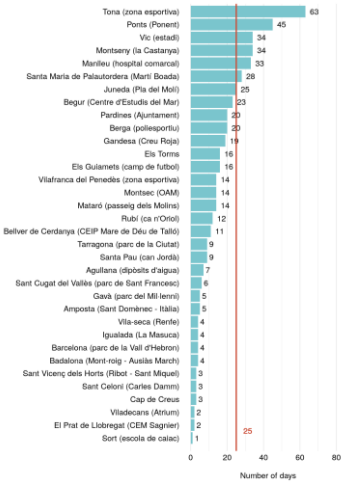

(q) 2018

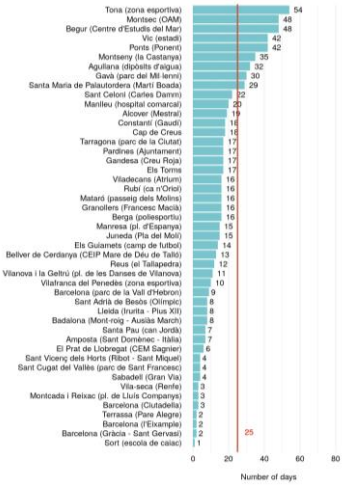

(r) 2020

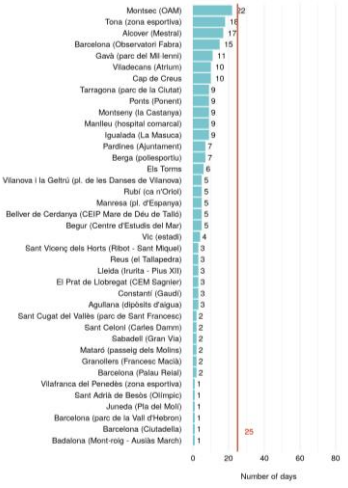

Figure S.2. NO_2 annual mean levels [µg/m^3] for background, industrial and traffic stations in Catalonia from 2000 to 2021. The grey horizontal lines show the annual mean thresholds set in the European Air Quality Directive (40 µg/m^3) and in the WHO guidelines (10 µg/m^3).

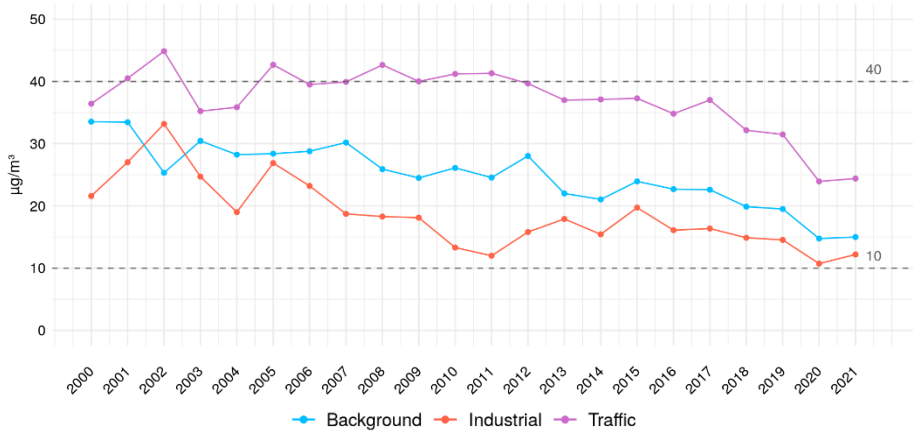

Figure S.3. Number of days per year exceeding the WHO recommended 100^{d8max} threshold at each air quality station in Catalonia in 2000-2018. Note that 3 days is the limit set in the WHO guidelines.

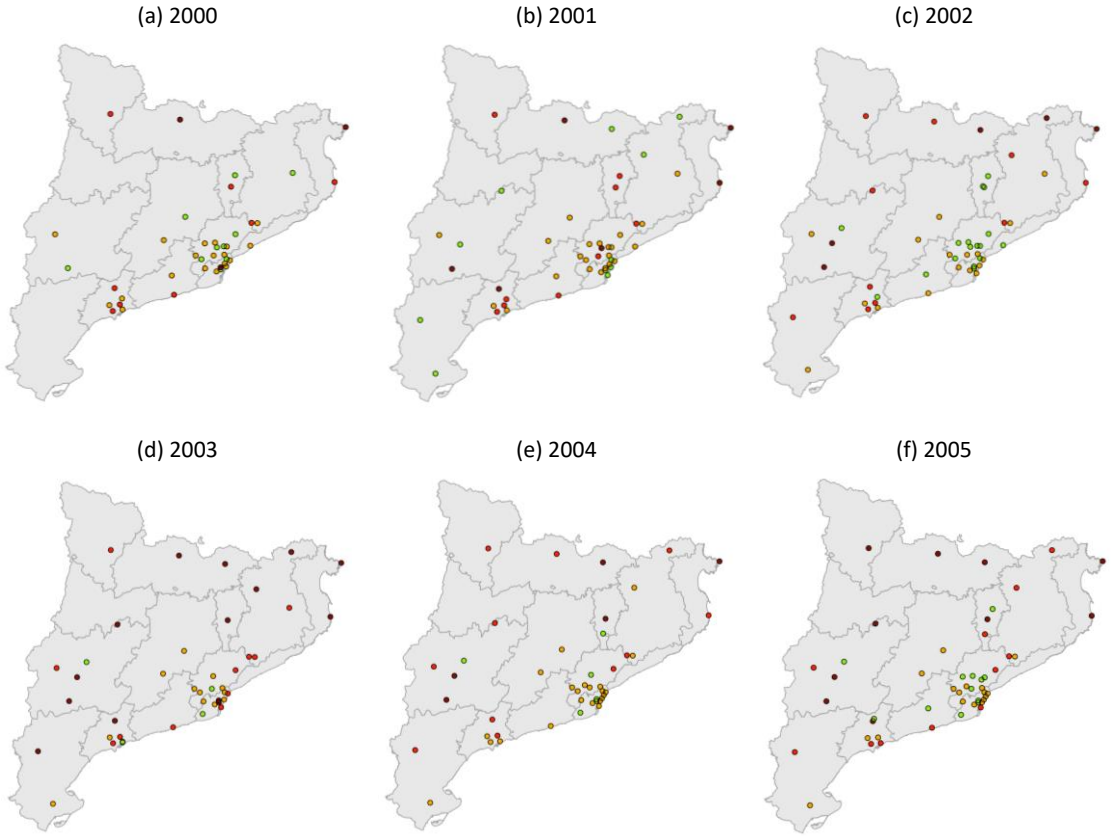

(g) 2006

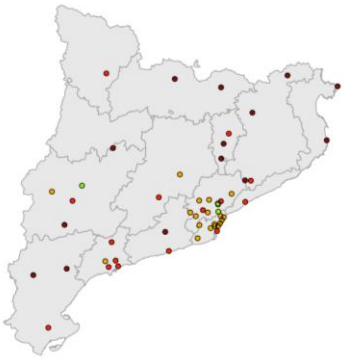

(h) 2007

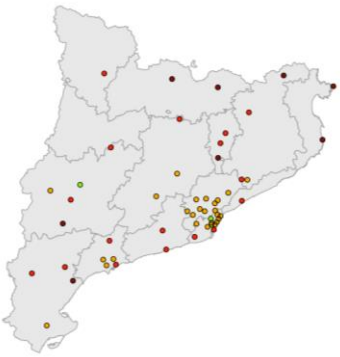

(i) 2008

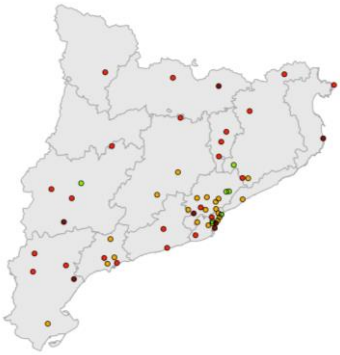

(j) 2009

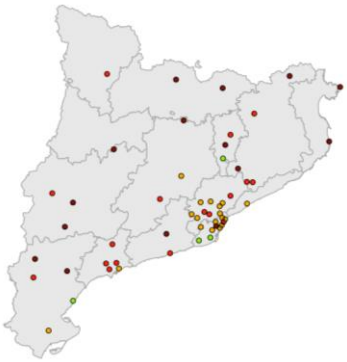

(k) 2010

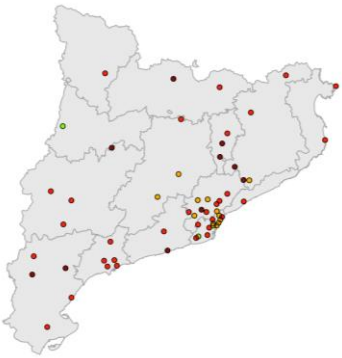

(l) 2011

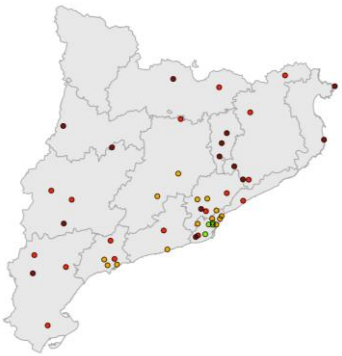

(m) 2012

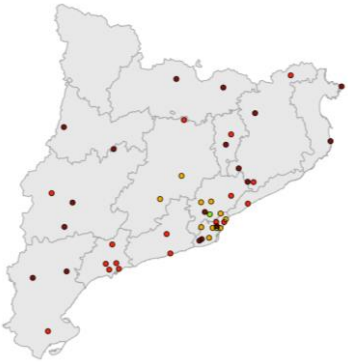

(n) 2013

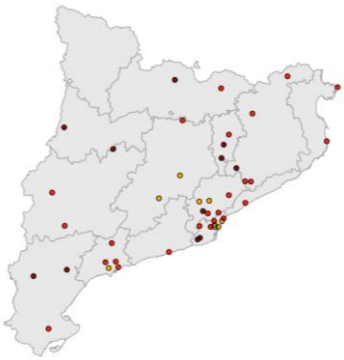

(o) 2014

(p) 2015

(q) 2016

(r) 2017

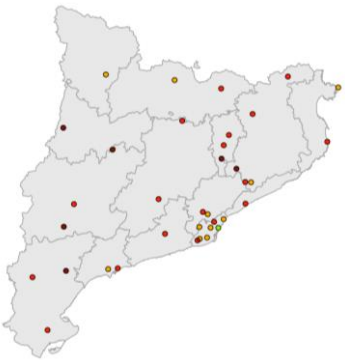

(s) 2018

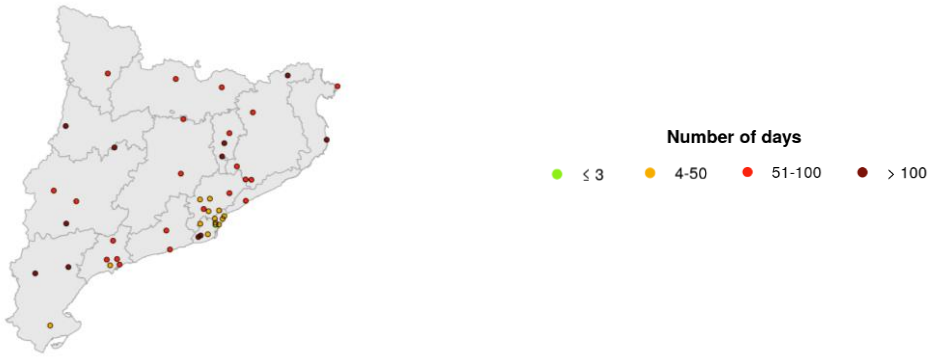

Figure S.4. Peak season O_3 concentration [µg/m^3] at each air quality station in Catalonia in 2000-2018. Note that 60 µg/m^3 is the peak season threshold set in the WHO guidelines (60$^{\text{peak season}}$).

(a) 2000 (b) 2001 (c) 2002

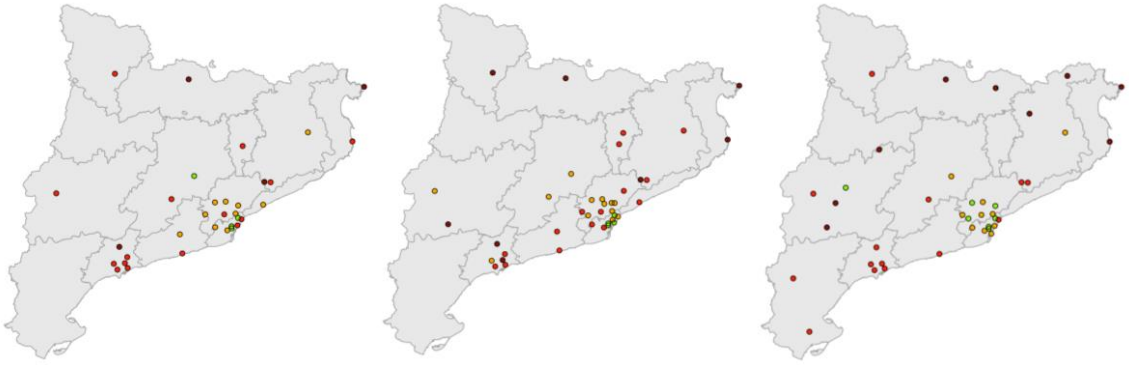

(d) 2003 (e) 2004 (f) 2005

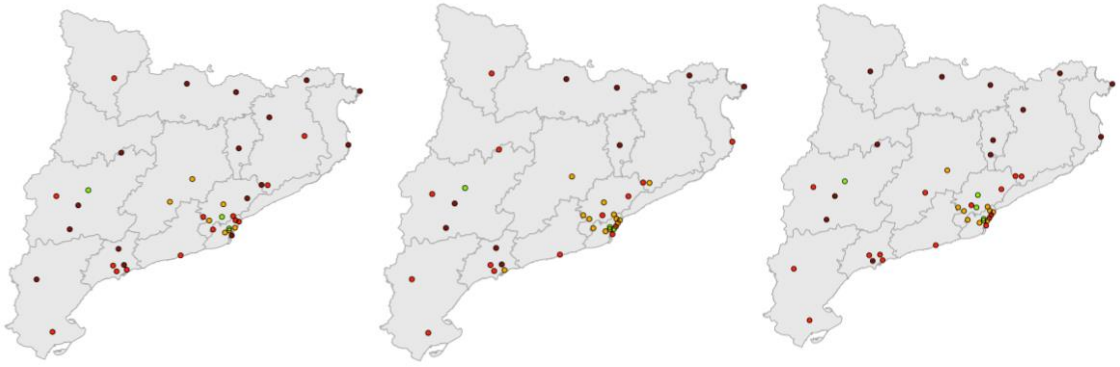

(g) 2006 (h) 2007 (i) 2008

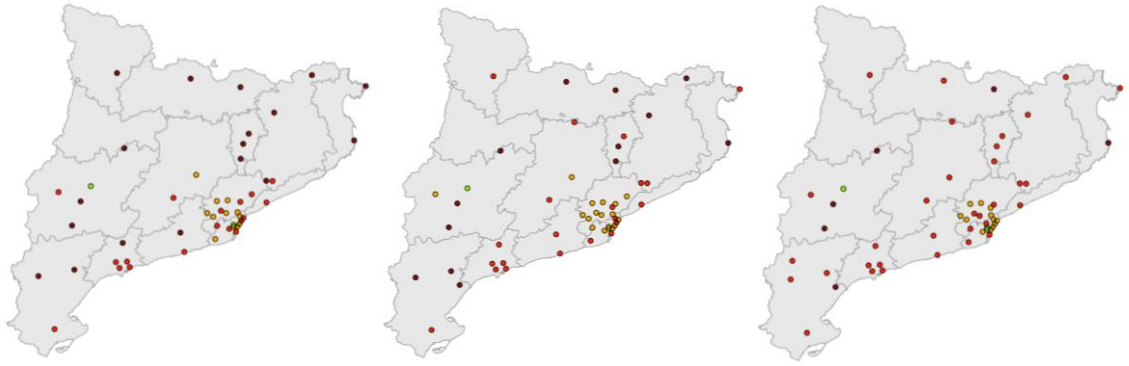

(j) 2009 (k) 2010 (l) 2011

(m) 2012 (n) 2013 (o) 2014

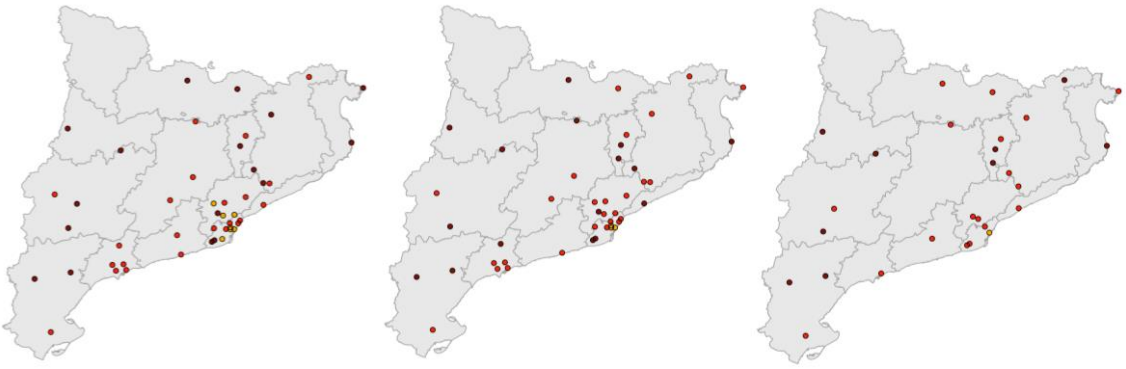

(p) 2015 (q) 2016 (r) 2017

(s) 2018

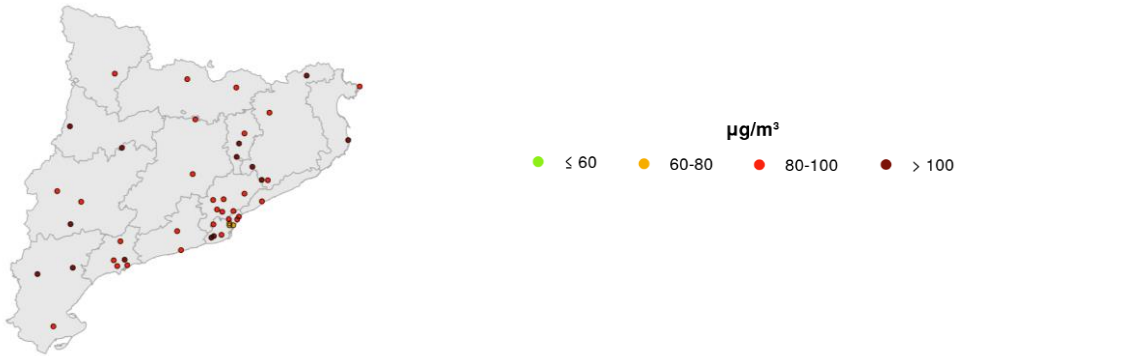

S.2. Evaluation of CALIOPE per station type

Table S.1. Evaluation of the model for BE1 and BE2 scenarios over April-September 2019 for the 50 available air quality stations in 2019, per station type, at different temporal scales: O_3^h, O_3^d, O_3^{d8max} and O_3^{d1max}. The statistics are mean bias (MB, µg/m^3), normalized mean bias (nMB, %), root mean square error (RMSE, µg/m^3), normalised root mean square error (nRMSE, %), Pearson correlation coefficient (PCC) and number of points (N).

Type of station	Scenario	Temporal scale	MB	nMB	RMSE	nRMSE	PCC	N
Urban	BE1	O_3^h	27.93	45.67	35.54	58.11	0.70	70272
Urban	BE1	O_3^d	28.10	46.03	31.19	51.09	0.59	2928
Urban	BE1	O_3^{d8max}	22.49	25.71	27.37	31.30	0.59	2928
Urban	BE1	O_3^{d1max}	19.78	20.33	27.07	27.82	0.58	2928
Urban	BE2	O_3^h	26.15	42.76	34.46	56.34	0.68	70272
Urban	BE2	O_3^d	26.32	43.11	29.67	48.58	0.56	2928
Urban	BE2	O_3^{d8max}	19.13	21.87	25.07	28.67	0.54	2928
Urban	BE2	O_3^{d1max}	16.50	16.95	24.97	25.66	0.55	2928
Suburban	BE1	O_3^h	27.59	41.38	36.85	55.27	0.66	74664
Suburban	BE1	O_3^d	27.61	41.42	31.49	47.24	0.52	3111
Suburban	BE1	O_3^{d8max}	16.43	17.29	22.31	23.48	0.58	3111
Suburban	BE1	O_3^{d1max}	13.24	12.66	22.06	21.09	0.62	3111
Suburban	BE2	O_3^h	22.67	34.00	32.63	48.94	0.69	74664
Suburban	BE2	O_3^d	22.69	34.03	26.89	40.34	0.56	3111
Suburban	BE2	O_3^{d8max}	11.92	12.55	19.55	20.57	0.54	3111
Suburban	BE2	O_3^{d1max}	8.83	8.44	20.05	19.17	0.59	3111
Rural	BE1	O_3^h	22.86	29.41	32.49	41.80	0.60	74664
Rural	BE1	O_3^d	22.90	29.46	27.61	35.52	0.59	3111
Rural	BE1	O_3^{d8max}	12.32	12.37	18.11	18.19	0.67	3111
Rural	BE1	O_3^{d1max}	10.35	9.62	18.51	17.21	0.70	3111
Rural	BE2	O_3^h	18.64	23.99	29.76	38.30	0.60	74664
Rural	BE2	O_3^d	18.66	24.01	24.37	31.35	0.57	3111
Rural	BE2	O_3^{d8max}	6.79	6.82	15.77	15.84	0.60	3111
Rural	BE2	O_3^{d1max}	4.09	3.80	16.58	15.42	0.65	3111

S.3. Characterisation of O_3 episodes in 2019

Here, we provide a characterisation of the three O_3 episodes that occurred in Catalonia in 2019, including a meteorological analysis. Due to similarities in terms of meteorology, we describe Episodes A and B together, whereas Episode C will be treated separately.

S.3.1. Episode A (28-29 June) and Episode B (23 July)

Episode A occurred on 28 and 29 June, when the alert threshold was exceeded for a total of five hours at four air quality stations located in Comarques de Girona (2 hours in Montseny, 2 hours in Sant Celoni and 1 hour in Santa Maria de Palautordera) and Àrea de Barcelona (1 hour in Gavà). Nevertheless, from 27 June to 5 July, except 3 July, there were a total of 87 hours in which the information threshold was surpassed throughout Catalonia (Table S.2).

Table S.2. Summary of the characteristics of Episode A: alert threshold exceedances (ATEs; number of hours), number of stations with ATEs, information threshold exceedances (ITEs; number of hours), number of stations with ITEs, and air quality zones involved. The principal days of the episode are highlighted in orange. Here, we only consider those days exceeding the alert or information thresholds.

	Episode A							
Day	**27 June**	**28 June**	**29 June**	**30 June**	**1 July**	**3 July**	**4 July**	**5 July**
ATEs (nº of hours)	0	4	1	0	0	0	0	0
nº of stations with ATEs	0	3	1	0	0	0	0	0
ITEs (nº of hours)	5	22	45	1	1	1	3	9
nº of stations with ITEs	3	9	17	1	1	1	2	5
Air quality zones involved	Catalunya Central	Comarques de Girona	Àrea de Barcelona	Pirineu Oriental	Plana de Vic	Camp de Tarragona	Catalunya Central	Comarques de Girona
	Plana de Vic	Empordà	Catalunya Central				Pirineu Oriental	Plana de Vic
		Plana de Vic	Penedès - Garraf					
		Vallès - Baix Llobregat	Pirineu Oriental					
			Vallès - Baix Llobregat					

On the other hand, Episode B took place on 23 July, when the alert threshold was exceeded for two hours, each at a different station in Plana de Vic (Manlleu and Vic). Furthermore, from 22 to 26 July, a total of 23 hours above the information threshold were recorded in this region, in addition to Catalunya Central and Comarques de Girona (Table S.3).

Table S.3. Summary of the characteristics of Episode B: alert threshold exceedances (ATEs; number of hours), number of stations with ATEs, information threshold exceedances (ITEs; number of hours), number of stations with ITEs, and air quality zones involved. The principal day of the episode is highlighted in orange. Here, we only consider those days exceeding the alert or information thresholds.

	Episode B			
Day	22 July	23 July	24 July	26 July
ATEs (nº of hours)	0	2	0	0
nº of stations with ATEs	0	2	0	0
ITEs (nº of hours)	4	10	6	3
nº of stations with ITEs	3	4	3	2
Air quality zones involved	Catalunya Central	Comarques de Girona	Catalunya Central	Plana de Vic
	Plana de Vic	Plana de Vic	Plana de Vic	

Regarding the synoptic meteorology, Episodes A and B were characterised by surface anticyclones situated over Western Europe, in addition to a low pressure gradient over Catalonia (Figure S.5). This situation led to stagnant conditions, clear skies and high temperatures, which are typical elements that enhance O_3 production (Pay et al., 2019). Therefore, the meteorological conditions during both events were optimal for high O_3 levels.

In fact, Episodes A and B coincided in time with the only two heat waves that the competent authorities declared in 2019 in Catalonia. The first occurred between 25 and 30 June, while the second from 22 to 25 July (Servei Meteorològic de Catalunya, 2021).

Figure S.5. 500 hPa geopotential height [dam] (coloured background) and ground-level pressure [hPa] (solid white lines) on 28 June, 29 June and 23 July at 12h UTC, according to Climate Forecast System Reanalysis (Wetterzentrale, 2023).

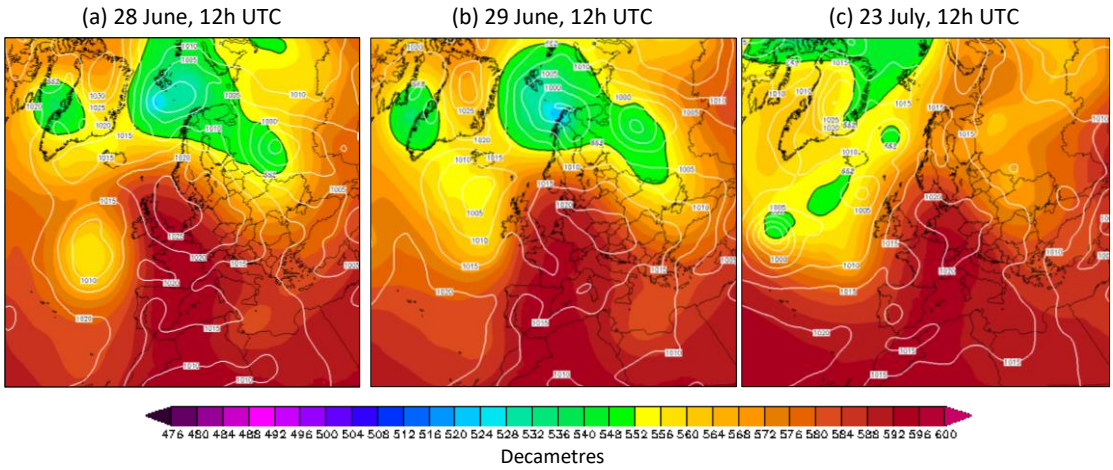

In summer, when there is a lack of a marked synoptic advection and stagnant conditions prevail, as occurred during Episodes A and B, flow is controlled by mesoscale phenomena. Hence, sea breezes are highly developed and long-range advection of air masses is not remarkable.

Sea breezes tend to follow a diurnal cycle (at surface level, from sea to land during solar hours and the opposite at night), which might lead to the recirculation of pollutants. Thus, during daytime, inland breeze circulations may transport O_3 precursors from the coast to inland stations (Jaén et al., 2021). In addition, several valleys crossing the coastal Catalan ranges favour the transport of pollutants from the BMA, which constitutes the most important source of NO_x and VOCs in Catalonia, to inland cities such as Vic (through the Besòs-Congost rivers valley) or

Manresa (through the Llobregat river valley) (Jaén, 2020). This phenomenon might be appreciated in Figure S.6 and Figure S.7. They represent the wind speed and direction at the automatic weather stations of the XEMA network (*Xarxa d'Estacions Meteorològiques Automàtiques*) a few hours before the alert threshold was exceeded at the affected stations on the main days of Episodes A and B, respectively.

Figure S.6. Wind speed [km/h] and direction at XEMA's automatic stations on 28 and 29 June at 11:00-11:30h UTC (Servei Meteorològic de Catalunya, 2023).

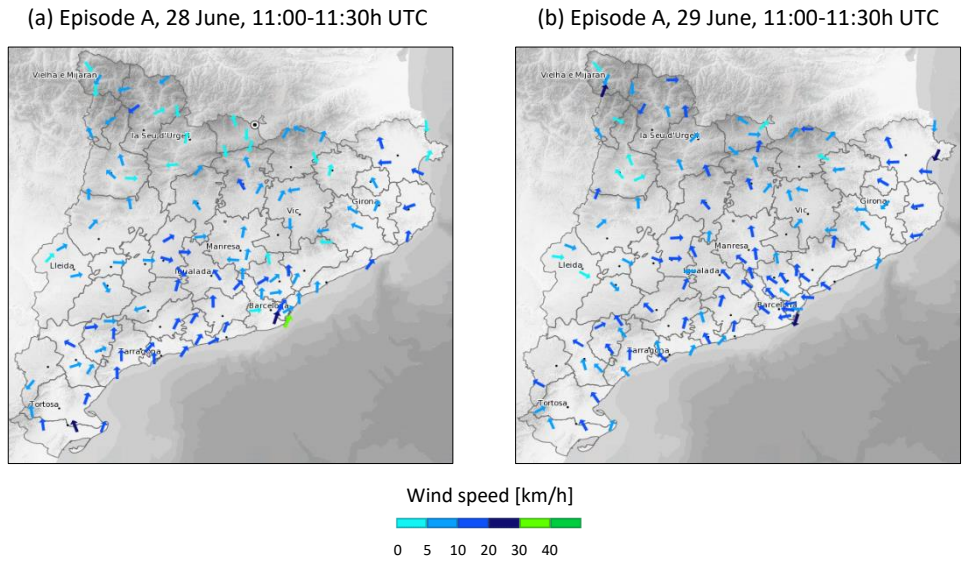

Figure S.7. Wind speed [km/h] and direction at XEMA's automatic stations on 23 July at 11:00-11:30h UTC (Servei Meteorològic de Catalunya, 2023).

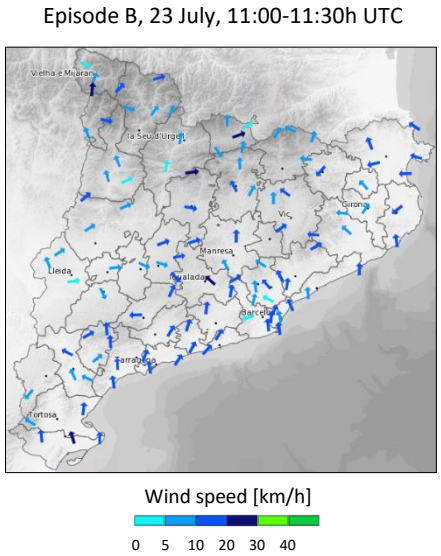

On the one hand, 28 June (Figure S.6a) and 23 July (Figure S.7) can be treated similarly: according to the wind direction, in both cases the diurnal breeze penetrated inland through the north-eastern valleys of Barcelona (Besòs-Congost pathway), moving towards Montseny and Plana de Vic, which were the most affected zones by O_3 levels on these two days. The breeze transported inland the O_3 precursors of the morning traffic rush hours from the BMA (28 June was Friday and 23 July was Tuesday). Accordingly, the maximum O_3 values evolved inland over time following the mentioned trajectory, as can be observed in Figure S.8 (28 June) and Figure S.9 (23

July). In fact, on 28 June, the first exceedances of the information threshold were recorded at 11h UTC in Rubí and Sant Celoni, which are relatively close to the high emission source area of Barcelona. Subsequently, peaks were observed at more inland stations such as Tona (at 14h UTC), Vic and Manlleu (at 15h UTC). These two events correspond to the typical O_3 episode affecting Plana de Vic characterised by many authors such as Querol et al. (2017) and Massagué et al. (2019).

Figure S.8. Observed and modelled O_3 concentrations [µg/m^3] in Catalonia for 28 June from 8h to 19h UTC (top: BE1; bottom: BE2). The shaded contour plot shows modelled values while the coloured dots correspond to the air quality station measurements.

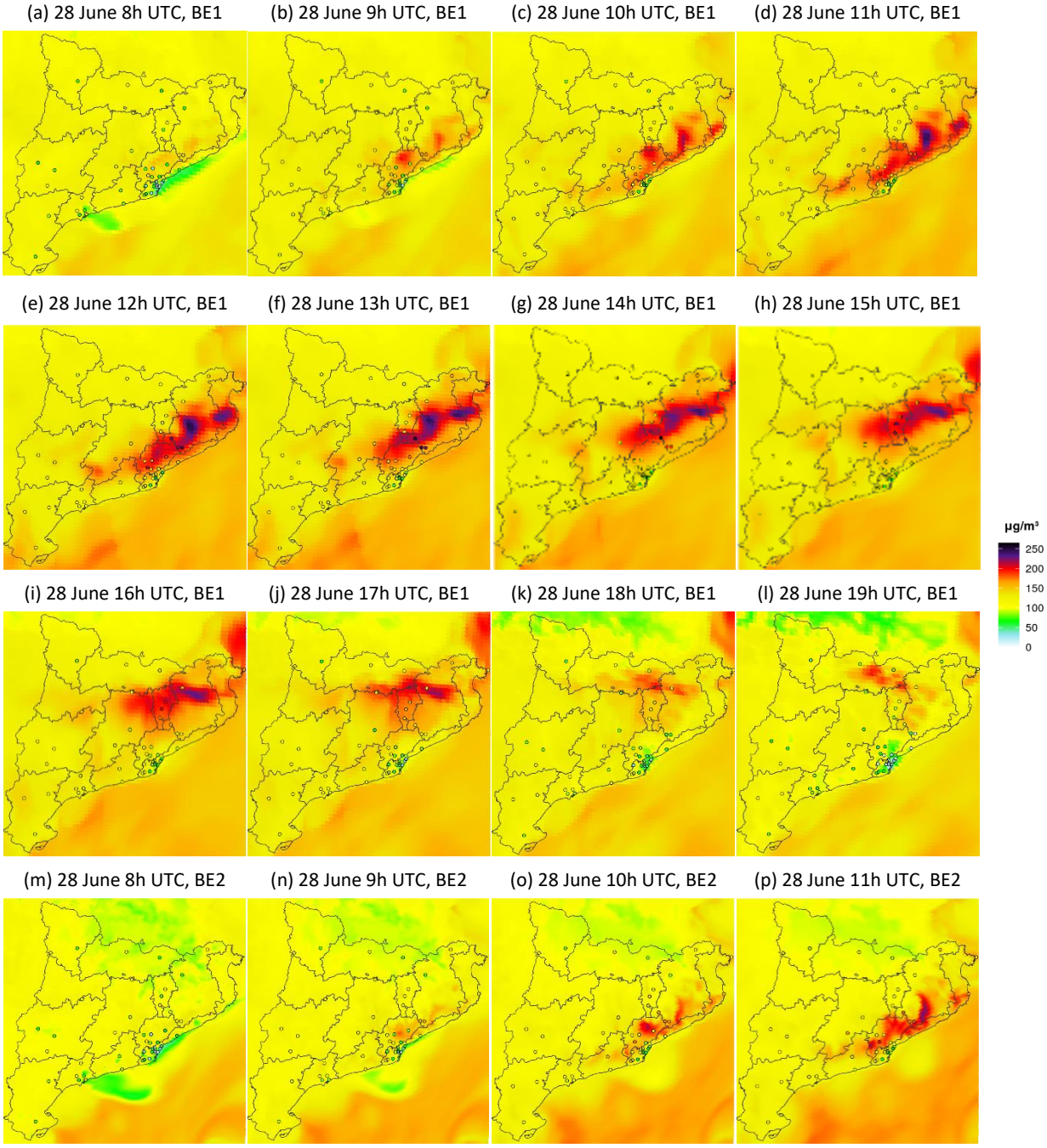

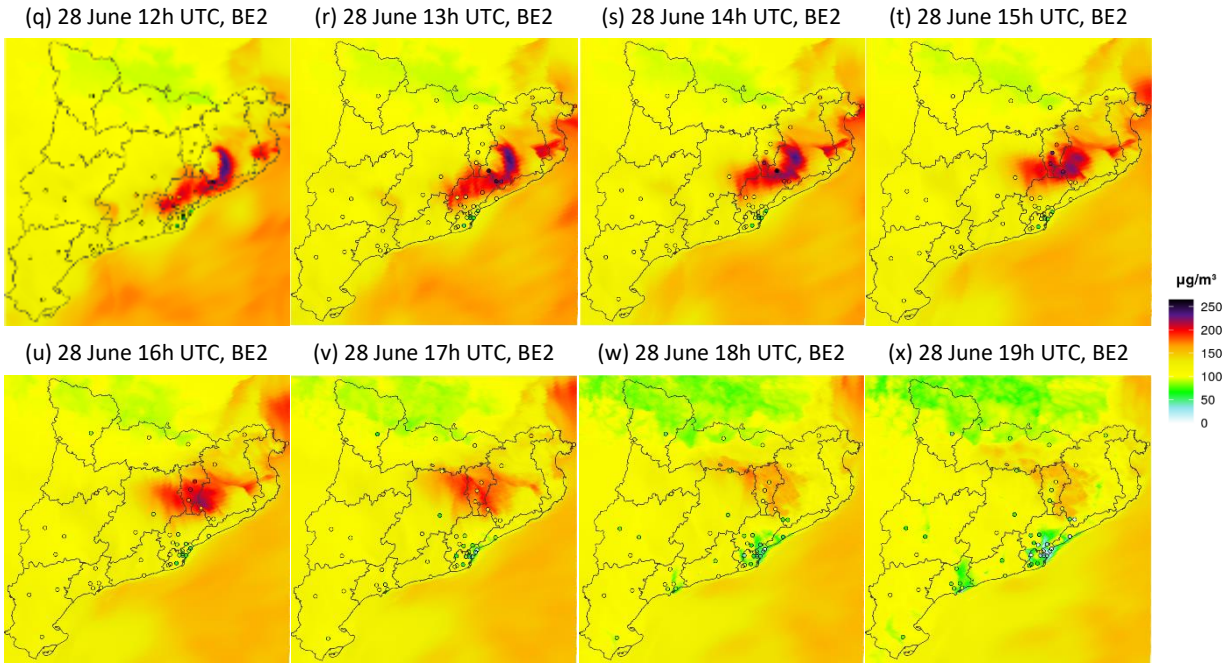

Figure S.9. Observed and modelled O_3 concentrations [µg/m^3] in Catalonia for 23 July from 8h to 19h UTC (top: BE1; bottom: BE2). The shaded contour plot shows modelled values while the coloured dots correspond to the air quality station measurements.

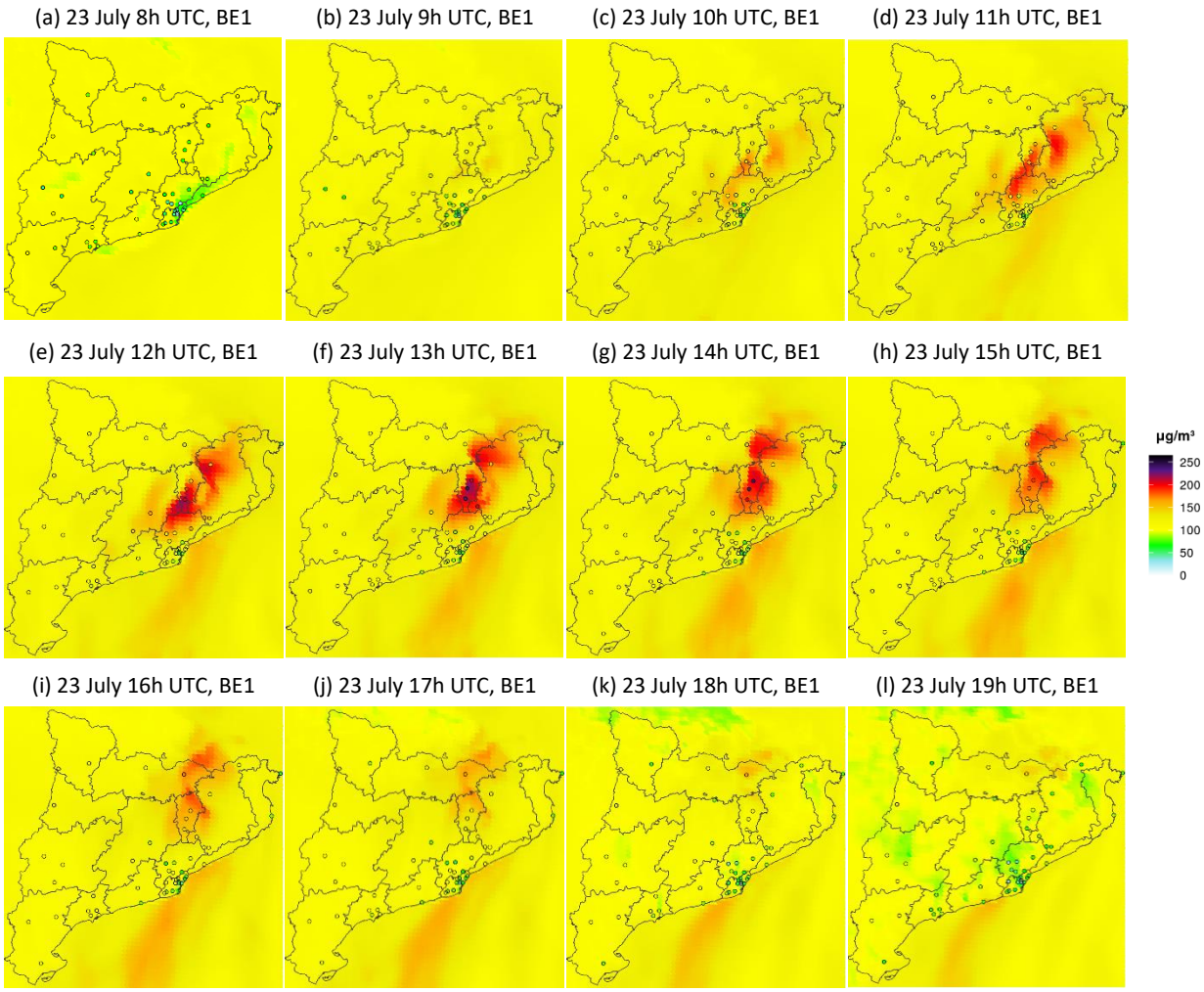

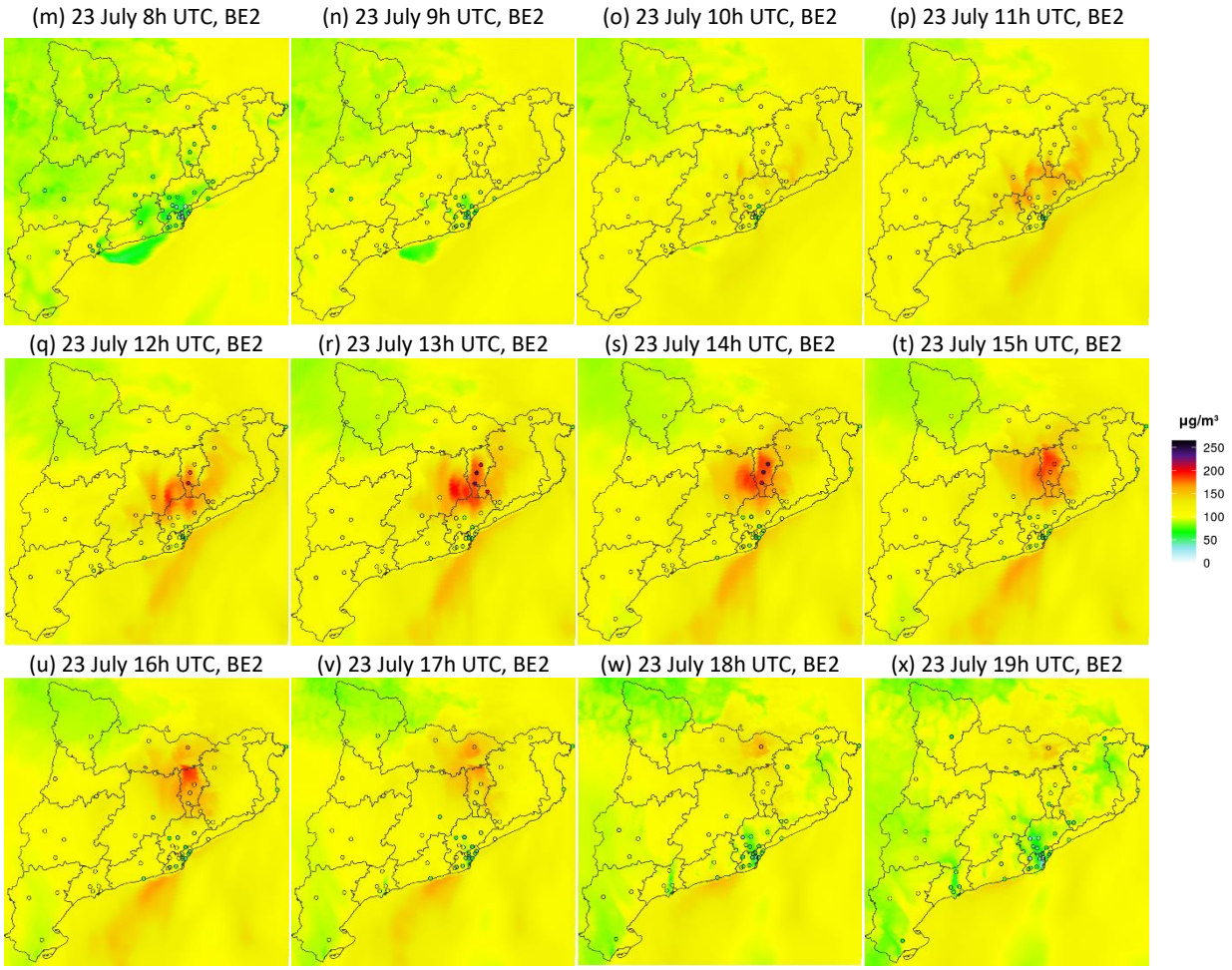

On the other hand, on 29 June (Figure S.10), the breeze followed the Llobregat river pathway and was directed towards the area of Manresa and Igualada, reasonably coinciding with the O_3 plume. In this case, the peak occurred first in Igualada at 13h UTC, and then in Manresa and Bellver de Cerdanya at 16 and 17h UTC, respectively. Considering that 29 June was Saturday, the weekend effect possibly contributed to this episode. This might explain the high O_3 concentrations seen in the BMA on 29 June. Therefore, the main contribution to the episode of 29 June could be due to recirculation rather than the influence of the emitted O_3 precursors (Jaén, 2020).

Apart from these exceedances, the air quality station in Gavà recorded O_3 levels over the 240^h limit on 29 June at 14h UTC. Considering that this city is slightly deviated from the Llobregat river trajectory, the origin of this peak is not so clear. It could be an example of the combination of the weekend effect, O_3 recirculation and O_3 fumigation, which occurs during the morning growth of the boundary layer that introduces O_3 from earlier days accumulated in high reservoir layers overnight and contributes to the increase in surface O_3 concentrations (Jaén et al., 2021). Moreover, the wind direction in the port of Barcelona during the hours prior to the peak was southwestward, towards Gavà and Llobregat valley, following an unusual direction. This implied advection from sea air layers but also from all the emissions resulting from the industrial activity of the port of Barcelona (Jaén, 2020).

Figure S.10. Observed and modelled O_3 concentrations [µg/m^3] in Catalonia for 29 June from 8h to 19h UTC (top: BE1; bottom: BE2). The shaded contour plot shows modelled values while the coloured dots correspond to the air quality station measurements.

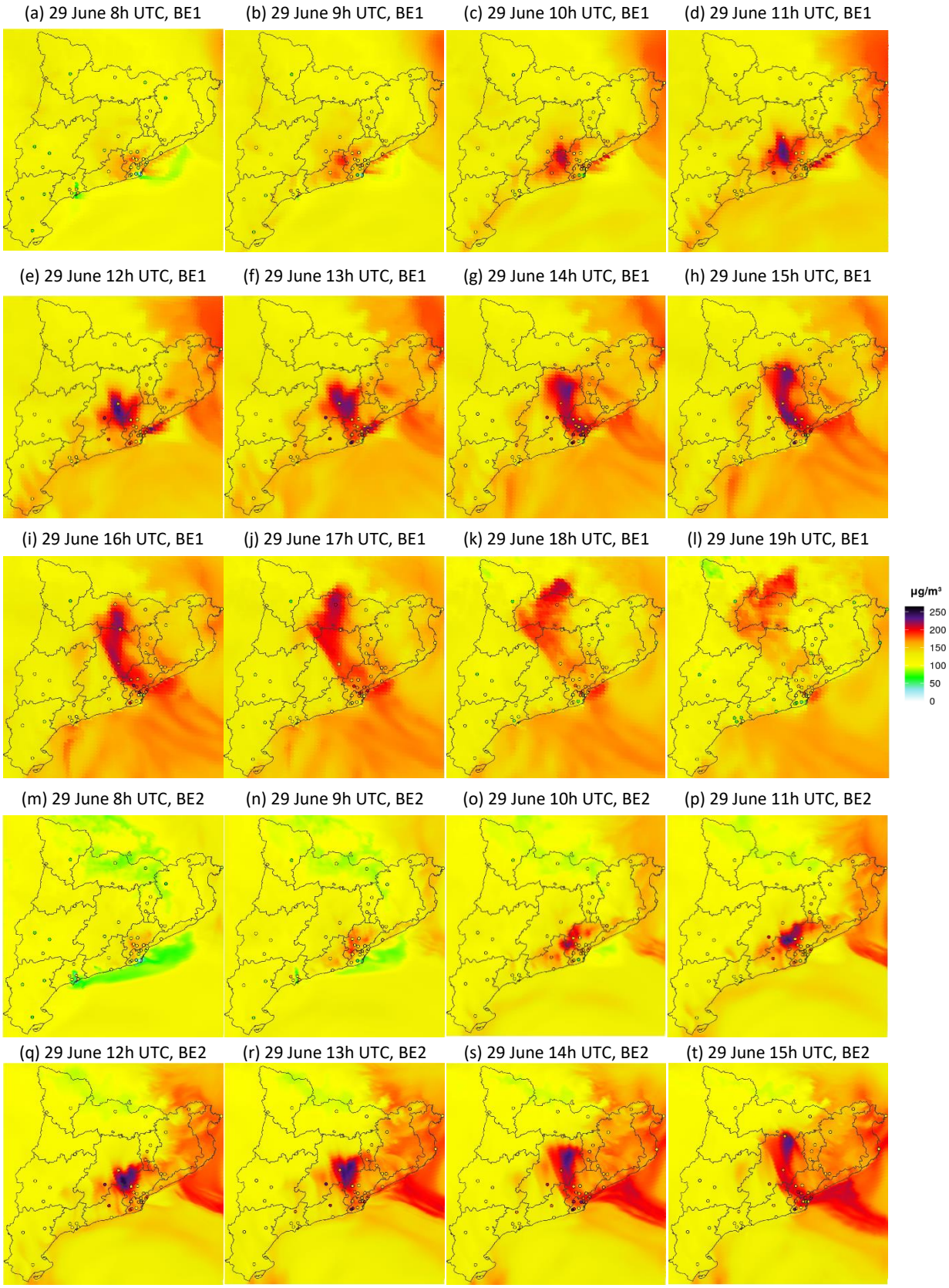

(u) 29 June 16h UTC, BE2 (v) 29 June 17h UTC, BE2 (w) 29 June 18h UTC, BE2 (x) 29 June 19h UTC, BE2

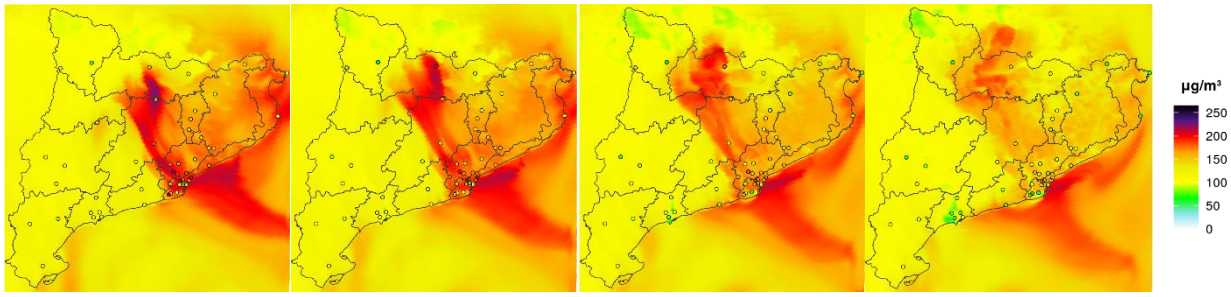

S.3.2. Episode C (18 September)

Episode C occurred on 18 September, but took place on a more local scale: it only affected the southern part of Camp de Tarragona air quality zone Figure S.11). During this day, there was an exceedance of the alert threshold in Tarragona city, and four exceedances of the information threshold in the latter and in Vila-seca (Table S.4).

Figure S.11. Observed and modelled O_3 concentrations [µg/m^3] in Catalonia for 18 September from 9h to 14h UTC (top: BE1; bottom: BE2). The shaded contour plot shows modelled values while the coloured dots correspond to the air quality station measurements.

(a) 18 September 9h UTC, BE1 (b) 18 September 10h UTC, BE1 (c) 18 September 11h UTC, BE1

(d) 18 September 12h UTC, BE1 (e) 18 September 13h UTC, BE1 (f) 18 September 14h UTC, BE1

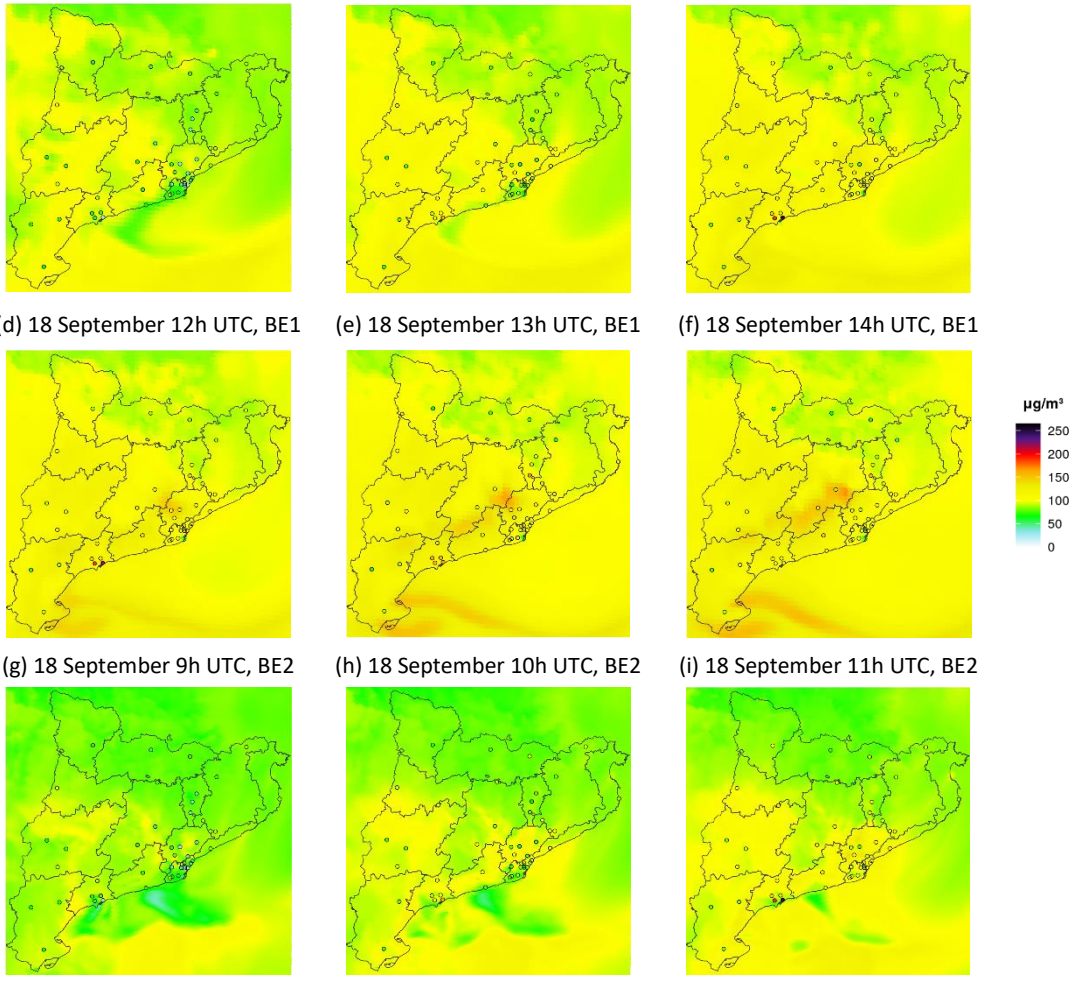

(g) 18 September 9h UTC, BE2 (h) 18 September 10h UTC, BE2 (i) 18 September 11h UTC, BE2

(j) 18 September 12h UTC, BE2 (k) 18 September 13h UTC, BE2 (l) 18 September 14h UTC, BE2

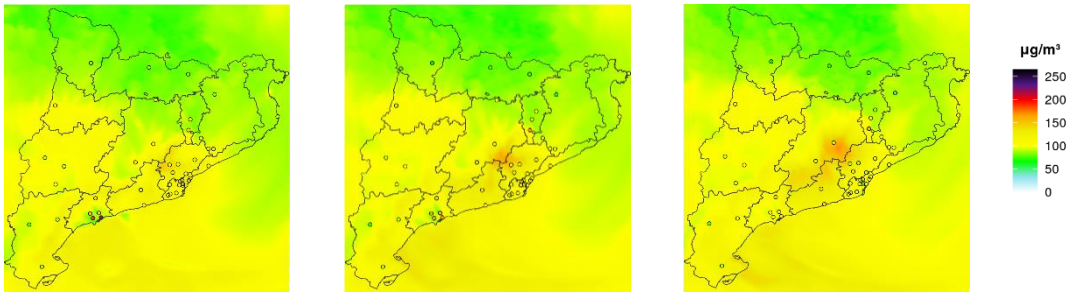

Table S.4. Summary of the characteristics of Episode C: alert threshold exceedances (ATEs; number of hours), number of stations with ATEs, information threshold exceedances (ITEs; number of hours), number of stations with ITEs, and air quality zones involved. The principal day of the episode is highlighted in orange. Here, we only consider those days exceeding the alert or information thresholds.

	Episode C
Day	18 September
ATEs (nº of hours)	1
nº of stations with ATEs	1
ITEs (nº of hours)	4
nº of stations with ITEs	2
Air quality zones involved	Camp de Tarragona

During Episode C, the synoptic situation was similar to that of Episodes A and B, although in this case pressures and temperatures were lower. Nevertheless, the low pressure gradient in Catalonia visible in Figure S.12 also led to stagnant conditions and a greater predominance of mesoscale phenomena.

Figure S.12. 500 hPa geopotential height [dam] (coloured background) and ground-level pressure [hPa] (solid white lines) on 18 September at 12h UTC, according to Climate Forecast System Reanalysis (Wetterzentrale, 2023).

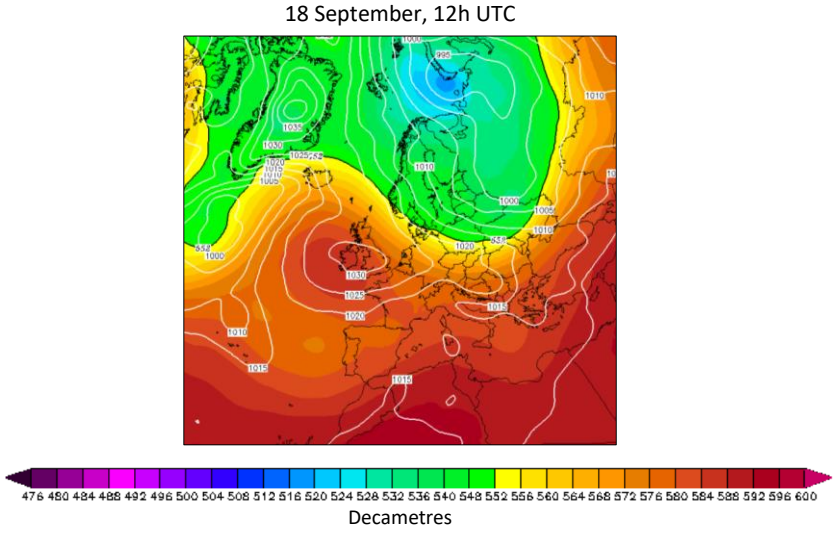

The origin of Episode C in Tarragona is unclear, as it occurred on a local scale and only affected the two stations near the coastline of Tarragona, but it could be due to a combination of different causes: (i) the usual high levels of O_3 precursors in this area resulting from the petrochemical complex and the urban agglomeration; (ii) the existence of meteorological stagnation and relatively high temperatures (Servei Meteorològic de Catalunya, 2023) that enhanced O_3 formation and (iii) a possible breeze blockage that caused air masses that had been

accumulating overnight over the Mediterranean, loaded with NO_x and O_3, to return to land on the morning of 18 September, when the sea breeze direction shifted (Figure S.13).

Figure S.13. Wind speed [km/h] and direction at XEMA's automatic stations on 18 September at 4:00-4:30, 10:00-10:30, 10:30-11:00h UTC (Servei Meteorològic de Catalunya, 2023).

(a) 18 September, 6:30-7:00h UTC (b) 18 September, 9:30-10:00h UTC (c) 18 September, 10:00-10:30h UTC

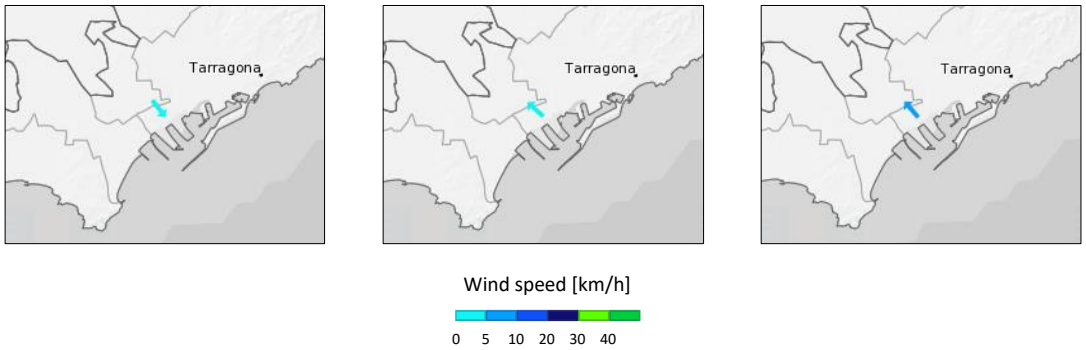

S.4. Impact of the emission abatement scenarios on the estimated O_3^{d8max} observations over the study period

Figure S.14 shows the mean estimated O_3^{d8max} observations for the abatement scenarios (Obs_Δ_PE_PNCCA and Obs_Δ_PE_BCN_UMP) against the base case measured observations (Obs), disaggregated temporally and per station type.

On the one hand, in the PE_PNCCA scenario (Figure S.14a) there are some reductions of the estimated O_3 observations (solid lines) against the base case measured observations (dashed lines). These reductions are more noticeable in June, July and August, which could be due to the combination of two aspects: first, in July and August, the absolute reduction in NO_x emissions between PE_PNCCA and BE1 is higher than in other months. Second, it is in these three months when photochemical activity is greater, since temperatures are higher, thus more exceedances of O_3^{d8max} are reported (Table S.5) and, as stated in Section 7.3, it is in O_3 episodes when there is more potential to reduce O_3 concentrations by reducing local emissions.

In Figure S.14a-b, it is remarkable the null reduction of O_3 concentrations in the April peak observed in the three types of stations. It could be that on those dates there was an O_3 intrusion from other countries, and therefore the decrease in emissions at the Spanish or local level would be insufficient to notice reductions in O_3 concentrations.

The highest reductions in mean O_3^{d8max} levels for PE_PNCCA occur in the rural stations (Figure S.14a). In this type of stations, some exceedances of the threshold established by European standards (120^{d8max}) would be avoided, e.g., in July and August. Nevertheless, this threshold would still be surpassed in some days of April, June and July. The limit recommended by the WHO (100^{d8max}), which is more restrictive, would still be exceeded on many occasions.

On the other hand, the averaged reductions in the estimated O_3 observations for the PE_BCN_UMP scenario (Figure S.14b) are minimal over the entire period analysed. This had already been mentioned, but here it is even more noticeable because the observations are averaged according to the type of station. The fact of considering all the stations in Catalonia implies that the reductions in O_3 levels that are achieved in some stations, although minimal, are offset by the increases that occur in others.

Figure S.14. Mean estimated O_3^{d8max} observations for the abatement scenarios (Obs_Δ_PE_PNCCA and Obs_Δ_PE_BCN_UMP, in solid lines) and the base case measured observations (Obs, in dashed lines) in the Catalan air quality stations, according to station type, from April to September 2019. The grey horizontal lines show the 120^{d8max} and 100^{d8max} limits established in the European Directive and the WHO guidelines, respectively.

(a) O_3^{d8max}, Obs_Δ_PE_PNCCA and Obs

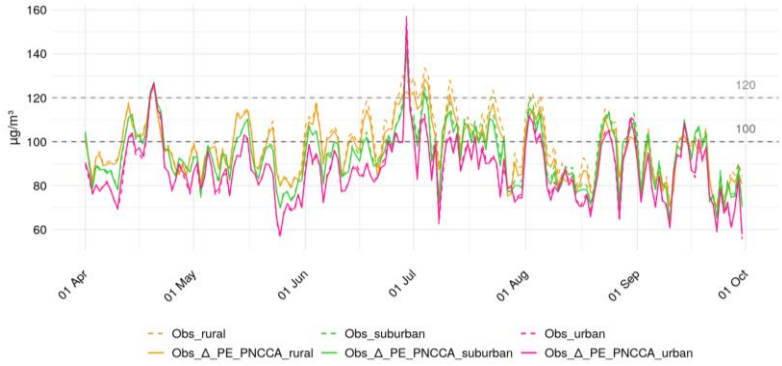

(b) O_3^{d8max}, Obs_Δ_PE_BCN_UMP and Obs

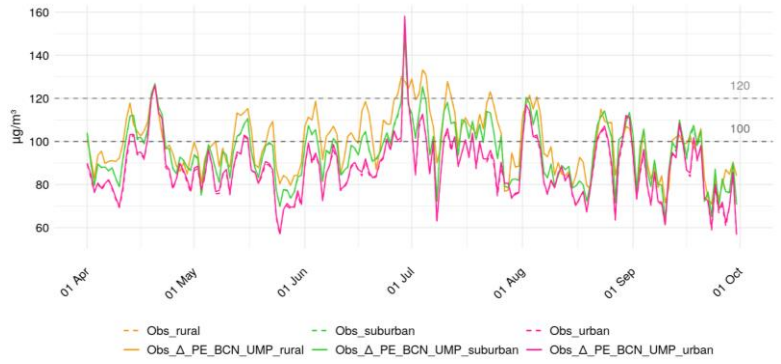

Table S.5. Number of exceedances of the target threshold (120^{d8max}) of the O_3 European standards at all stations of Catalonia from April to September 2019.

	Number of exceedances of the 120^{d8max} threshold
April	117
May	28
June	163
July	250
August	134
September	37

S.5. Sustainability analysis and ethical implications

Table S.6. Characteristics of the four emission simulations executed in the framework of this project and specifications of the MareNostrum 4 supercomputer.

	Value	Reference
Running time [h]	111.67	*
Type of cores	CPU	(BSC, 2018)
Number of computing cores	48	(Intel, 2022)
Thermal Design Power [W]	150	(Intel, 2022)
Memory available [GB]	96	(BSC, 2018)
Core usage factor	0.47	*
Power Usage Efficiency	1.08	(BSC, 2018)

*Obtained value in the executed simulations.

Equation S.1. Carbon footprint of computer energy consumption.

$$CF_{computer\ energy\ consumption} = 750\ h \cdot 0.5 \cdot 50W \cdot \frac{1kW}{10^3W} \cdot \frac{171g\ CO_2e}{1kWh} \cdot \frac{1kg\ CO_2e}{10^3g\ CO_2e} = 3.21kg\ CO_2e$$

Equation S.2. Carbon footprint of lighting energy consumption.

$$CF_{lighting\ energy\ consumption} = 750\ h \cdot 0.25 \cdot 60W \cdot \frac{1kW}{10^3W} \cdot \frac{171g\ CO_2e}{1kWh} \cdot \frac{1kg\ CO_2e}{10^3g\ CO_2e} = 1.92kg\ CO_2e$$

References

BSC (2018). *MareNostrum.* Retrieved 7 September, 2023, from https://www.bsc.es/es/marenostrum/marenostrum

Intel (2022). *Procesador Intel® Xeon® Platino 8160.* Retrieved 7 September, 2023, from https://www.intel.la/content/www/xl/es/products/sku/120501/intel-xeon-platinum-8160-processor-33m-cache-2-10-ghz/specifications.html

Jaén, C., Villasclaras, P., Fernández, P., Grimalt, J. O., Udina, M., Bedia, C., and van Drooge, B. L. (2021). Source apportionment and toxicity of PM in urban, sub-urban, and rural air quality network stations in Catalonia. *Atmosphere, 12*(6), 744. https://doi.org/10.3390/atmos12060744

Jaén, C. (2020). Oz Jaén, C. (2020). Ozone episodes in Catalonia during the summer of 2019. A meteorological and photochemical modeling analysis. *Dipòsit Digital de la Universitat de Barcelona*. Retrieved 26 May, 2023, from https://diposit.ub.edu/dspace/handle/2445/172706

Massagué, J., Carnerero, C., Escudero, M., Baldasano, J. M., Alastuey, A., and Querol, X. (2019). 2005–2017 ozone trends and potential benefits of local measures as deduced from air quality measurements in the north of the Barcelona metropolitan area. *Atmospheric Chemistry and Physics, 19*(11), 7445-7465. https://doi.org/10.5194/acp-19-7445-2019

Pay, M. T., Gangoiti, G., Guevara, M., Napelenok, S., Querol, X., Jorba, O., and Pérez García-Pando, C. (2019). Ozone source apportionment during peak summer events over southwestern Europe. *Atmospheric chemistry and physics, 19*(8), 5467-5494. https://doi.org/10.5194/acp-19-5467-2019

Querol, X., Gangoiti, G., Mantilla, E., Alastuey, A., Minguillón, M. C., Amato, F., Reche, C., Viana, M., Moreno, T., Karanasiou, A., Rivas, I., Pérez, N., Ripoll, A., Brines, M., Ealo, M., Pandolfi, M., Lee, H., Eun, H., Ahn, K. H. (2017). Phenomenology of high-ozone episodes in NE Spain. *Atmospheric Chemistry and Physics, 17*(4), 2817-2838. https://doi.org/10.5194/acp-17-2817-2017

Servei Meteorològic de Catalunya (2023). *Mapa d'estacions automàtiques*. Retrieved 21 June, 2023, from https://www.meteo.cat/observacions/xema?dia=2019-06-29T00:00Z

Servei Meteorològic de Catalunya (2021). *Butlletí climàtic anual del 2019.* Retrieved 16 May, 2023, from https://static-m.meteo.cat/wordpressweb/wp-content/uploads/2021/04/15125638/Butllet%C3%AD-clim%C3%A0tic-2019-v3.pdf

Wetterzentrale (2023). *GFS. Maps based on Global Forecast System of the US weather service.* Retrieved 21 June, 2023, from https://www.wetterzentrale.de/de/topkarten.php?model=gfs&lid=OP